Max-Planck-Institut
für Meteorologie

REPORT No. 268

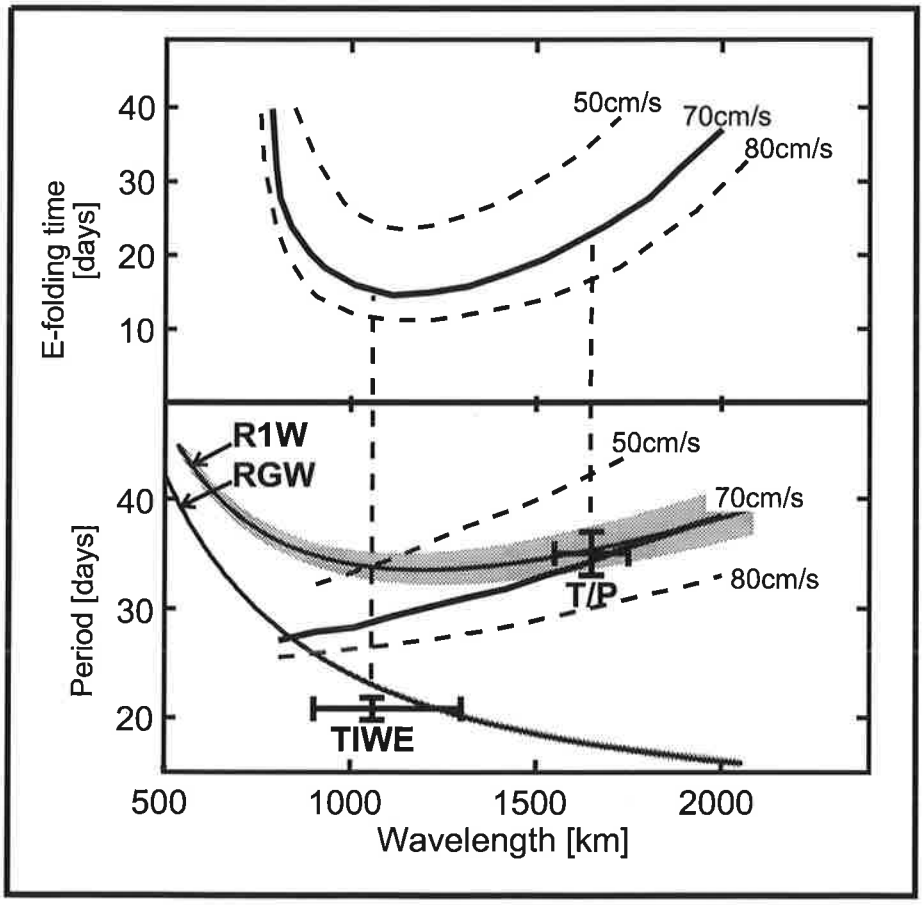

A NEW THEORY FOR TROPICAL INSTABILITY WAVES

by

Matthias Münnich • Mojib Latif

HAMBURG, July 1998

AUTHORS:

Matthias Münnich
Mojib Latif

Max-Planck-Institut
für Meteorologie

MAX-PLANCK-INSTITUT
FÜR METEOROLOGIE
BUNDESSTRASSE 55
D - 20146 HAMBURG
GERMANY

Tel.: +49-(0)40-4 11 73-0
Telefax: +49-(0)40-4 11 73-298
E-Mail: <name> @ dkrz.de

A New Theory for Tropical Instability Waves

Matthias Münnich and Mojib Latif

Max-Planck Institut für Meteorologie,
Bundesstr. 55,
D–20146 Hamburg,
Germany.

July 8, 1998

Science, submitted.

ISSN 0937–1060

Abstract

Large-scale westward propagating waves, so-called "Legeckis" or "Tropical Instability Waves", are a prominent feature of sea surface temperature images of the equatorial Pacific. Our analyses of satellite altimetry data and long-term moorings reveals that the Legeckis waves can be interpreted as a superposition of two distinct wave modes, a first equatorial Rossby wave and a Rossby-gravity wave. We present evidence that the energy sources for both waves are the mean currents. Our results imply that Legeckis waves can be explained within the framework of linear equatorial waves.

During boreal fall and winter large-scale wave structures are commonly visible in infra-red satellite images of the sea surface temperature in the equatorial Pacific (Fig. 1). These so-called "Legeckis" or "Tropical Instability Waves" (TIW) are observed a few degrees north of the equator between 100°W and the date line. The structure of these waves is quite variable. At some times TIW are symmetric about the equator (Fig. 1 B) while at others the waves are limited to the eastern Pacific (Fig.1 C). Estimates of the wavelengths and periods of the TIW vary from 900 to 2000 km and 20 to 40 days, respectively.

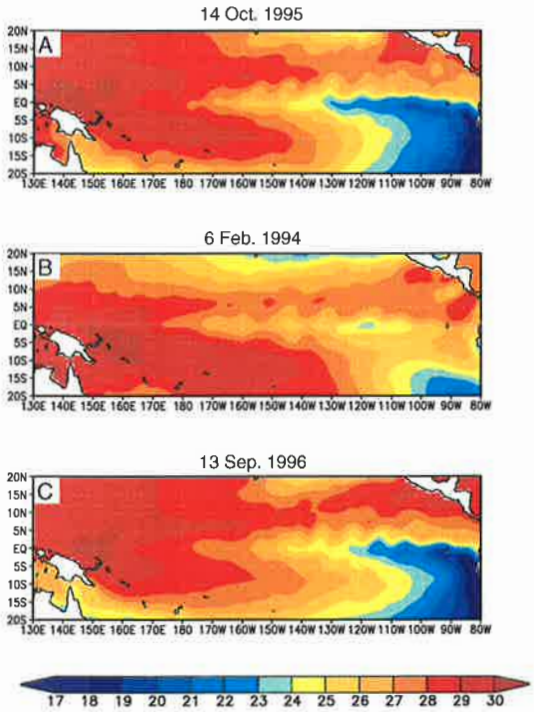

FIG. 1 Sea surface temperature (SST) snapshots derived from a combination of in-situ measurements and satellite data.

TIW have been extensively studied by satellites [1], [2], [3], in in-situ data [4], [5] and with ocean models [6], [7], [8]. An instability analysis of the equatorial current system revealed that the TIW do most likely obtain their energy from the shear of the mean currents [9]. The physics of these waves, however, remained somewhat obscure. Speculation on the nature of these waves range from wind-forced Rossby-gravity waves [10] or instability forced equatorial Rossby waves [11] to strongly nonlinear vortices [12] and equatorial Rossby solitons [13].

To investigate the dynamics of TIW we used primarily Topex/Poseidon (T/P) altimeter data processed by the French "Centre Localisation Satellite" (CLS). CLS provided us with maps of global sea level anomalies (SLA) at 10 day intervals [14].

A longitude – time section along 6°N (Fig. 2 A) of the T/P SLA data shows wave signals moving westward superimposed on the annual cycle. The location of these wave signals coincides with the region of strong meridional shear between the South Equatorial Current and the North Equatorial Countercurrent. TIW (see Fig. 1) are often observed in this region and these signals have been described in SLA observations [15].

A peak in the spatial mean of the frequency spectra of the T/P SLA data along 6°N yields a period of 35 ± 3 days and the corresponding time average of the wave number spectra a wavelength of 1650 ± 150 km, which results in a mean westward phase velocity of 55 cm/s. These values are consistent with earlier, less precise sea level satellite measurements [16], [15]. However, these wavelengths and periods for TIW are significantly larger than those based on SST and velocity measurements which are typically 1000 km and 21 days [17].

In order to double-check our results, we analyzed additionally daily temperature observations of the "Tropical Atmosphere Ocean" (TAO) moorings [18]. From these data we computed isotherm depths time series (Fig. 3). The correlation of the 20°C isotherm depth series derived from the TAO moorings with SLA at 140°W, 6°N amounts to 0.72. The spectrum of the isotherm depth series at 140°W, 6°N has the same peak at 35 days as the T/P SLA data. More importantly, we did not find any time lag between the T/P SLA data and the isotherm depth time series.

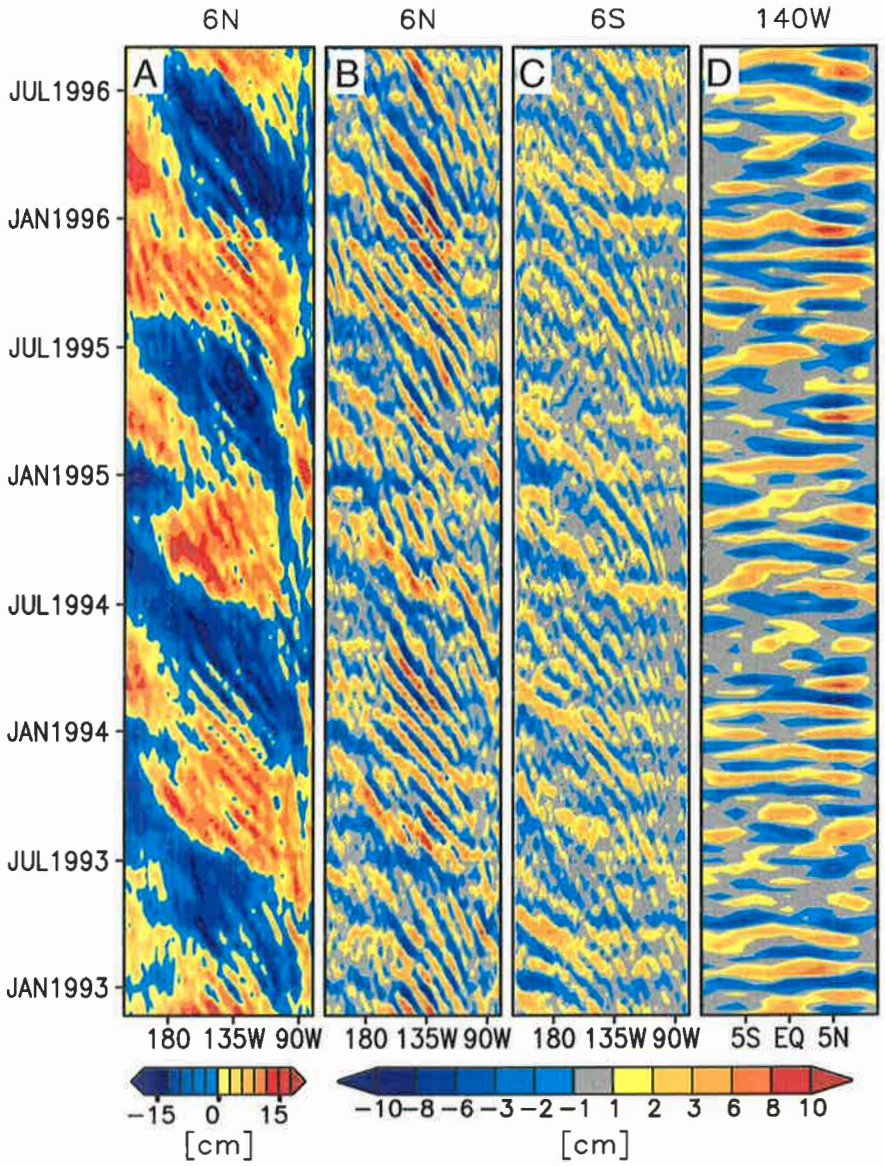

FIG. 2 Longitude-time and latitude-time sections of the Topex/Poseidon sea level anomaly (SLA) data. **A**, Anomalies along 6°N; **B, C** and **D**, High-pass filtered SLA —along 6°N, 6°S, and 140°W, respectively.

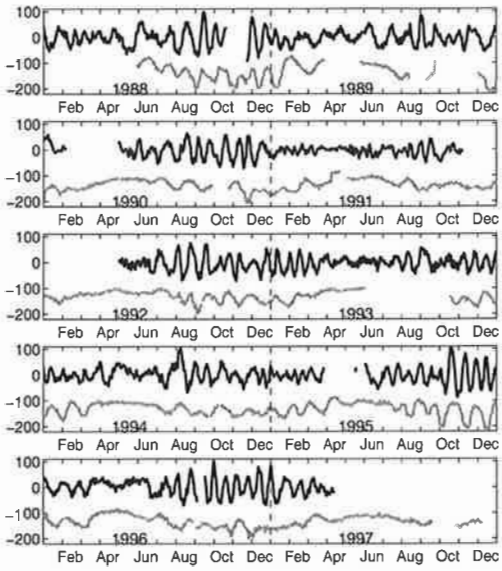

FIG. 3 Time series of the meridional velocity v in 25 m depth at the equator and 140°W (black, [cm/s]) and of the depth of the 20°C isotherm at 6°N, 140°W (gray, [m]).

We also confirmed the phase velocity estimate by computing the lag correlation function between the 20°C isotherm depth time series at 140°W, 5°N and 155°W, 5°N. The maximum correlation (0.4) is reached at a lag of 36 days. This corresponds to a signal velocity of 54 cm/s, which is in good agreement with our phase velocity estimate from the T/P data. Thus, our estimates of the characteristic space and time scales of the TIW are rather robust.

In order to highlight the TIW we applied a high-pass filter to the T/P data by subtracting at each grid point a nine point triangular moving average. The characteristic westward propagation exists not only to the north of the equator but also to the south of it (Fig. 2 B and 2 C). Furthermore, the signals north and south of the equator vary in phase over the whole latitude band 8°S – 8°N (Fig.2 D). This demonstrates that the signals north and south of the equator are part of the same wave motion. Its latitudinal structure with two maxima at 5°N and 5°S resembles the structure of a first mode equatorial Rossby wave (R1W, Fig. 4 B).

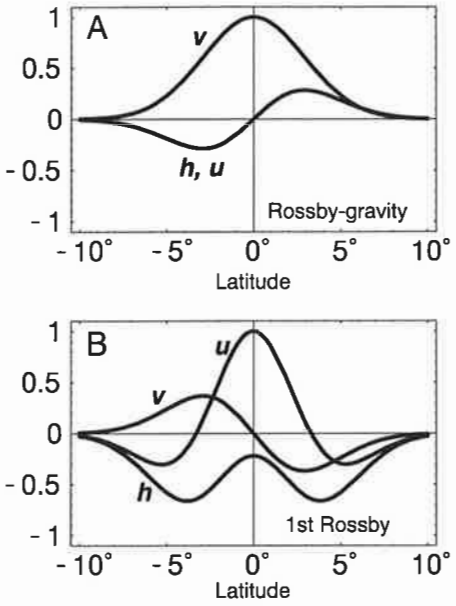

FIG. 4 Latitudinal structure function of the RGW and R1W. Meridional velocity v, longitudinal velocity u and surface elevation h.

Moreover, our wavelength and period estimates fit perfectly into the dispersion relation of these waves (red cross marked "T/P" in Fig. 5). The wavelength and period are exactly at the intersection of the R1W dispersion relation with the dispersion relation obtained from a barotropic instability analysis of the equatorial current system (black lines in Fig. 5, [9]). All these facts prove that TIW are in fact not the most unstable wave but are a free mode, the R1W. The period and wavelength of the R1W are determined by the values for which the wave mode can most efficiently draw energy from the mean current shear by barotropic instability.

As mentioned above our estimates for period and wavelength are larger than the common values found in the literature. The more precise of these earlier observations were obtained from in-situ velocity measurements within 2°of the equator and reported TIW in the meridional near surface velocity (v). Fig. 3 shows the time series of v at the equator at 140°W and the 20°C isotherm depth time series at 5°N as derived from the TAO array. It is obvious that these two oscillations are distinct: The oscillations in v are much faster with a mean period here is 21 days, consistent with a recent report [17] which estimated the wavelength of these waves as 900–1300 km.

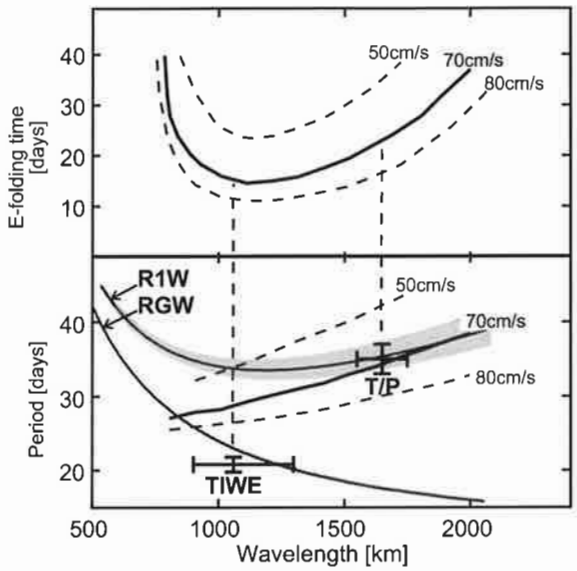

FIG. 5 E-folding times and periods of unstable waves computed with a 1.5 layer model [9]. The lines are labeled by the maximum velocity of the mean background current. The dispersion relations for Rossby-gravity wave and the first equatorial Rossby wave are labeled RGW and and R1W, respectively. The region where the assumed gravity wave velocity c_g for the dispersion relation falls within 2.2 cm/s $\leq c_g \leq$ 2.6 cm/s is shaded. The crosses show the estimates for the T/P SLA waves in Fig. 2 and TIW observed in the meridional velocity at the equator (labeled TIWE) [17].

Our classification of the T/P SLA waves as a first mode Rossby wave suggests an interpretation of the wave at the equator as another free mode. Indeed, the period and wavelength are in agreement with the dispersion relation of a Rossby-Gravity wave (RGW) (Fig. 5). The fact that the observed wave is mainly observed in v at the equator strengthens this interpretation, since v is strongest at the equator for this particular wave mode (Fig. 4).

The SST observations (Fig. 1) also support our wave scenario. Fig. 1 shows three snapshots of SST derived from a joint analysis of satellite, ship and mooring measurements [19]. The SST is expected to vary in phase with the movement of the isotherm. The R1W was well excited while the RGW was weak in Feb. 1994 (Fig. 3), so that the symmetry of the R1W in the h field about the equator (Fig. 4 B) is reflected in the observed SST. In contrast the RGW was strong while the R1W was nearly absent in Sep. 96 (Fig. 3, Fig. 1 C). At this time no symmetry exists in the SST just as predicted from the theoretical structure function for h of an RGW (Fig. 4 A).

Furthermore, the waves in Fig. 1 C are more confined to the eastern part of the Pacific compared with Fig. 1 B. This property can be explained by the different directions of

energy propagation given by the group velocities of R1W and RGW. The group velocity is always eastward for an RGW, while it is slowly westward for the observed wavelength of the R1W. Therefore the RGW can only exist east of its wave source.

Our interpretation of the TIW as free waves modes offers a very simple explanation for the large-scale current vortex observed in Nov. 1992 at 140°W, 5°N [12]. It was a very strong half-cycle of a R1W (see Fig. 3). Our wave theory provides also a new explanation for the large range of observed periods and wavelengths of the TIW in the literature, although the individual spectral peaks of the R1W and RGW are rather narrow. The superposition of both waves in the SST observations smeared the individual spectral peaks.

In summary, the basic dynamics of the observed Tropical Instability Waves (TIW) in the Pacific can be understood within the framework of free equatorial waves.

Acknowledgments

We like to thank D. Müller for many valuable suggestions. This work was sponsored by the European Union via the DUACS project (ENV4-CT96-0357).

References

1. R. Legeckis. Long waves in the eastern Equatorial Pacific Ocean. *Science*, **197**, 1179–1181, 1977.

2. M. R. Allen, S. P. Lawrence, M. J. Murray, C. T. Mutlow, T. N. Stockdale, D. T. Llewellyn-Jones, and D. L. T. Anderson. Control of tropical instability in the Pacific. *Geophys. Res. Let.*, **22**, 2581–2584, 1995.

3. E. J. Katz. Waves along the Equator in the Atlantic. *J. Phys.Oceanogr.*, **27**, 2536–2544, 1997.

4. D. Halpern, R. A. Knox, and D. S. Luther. Observation of 20-day period meridional current oscillations in the upper ocean along the Pacific equator. *J. Phys.Oceanogr.*, **18**, 1514–1534, 1988.

5. R. H. Weisberg and T. J. Weingartner. Instability waves in the equatorial Atlantic Ocean. *J. Phys.Oceanogr.*, **18**, 1641–1657, 1988.

6. M. D. Cox. Generation and propagation of 30-day waves in a numerical model of the Pacific. *J. Phys.Oceanogr.*, **10**, 1168–1186, 1980.

7. S. G. H. Philander, W. J. Hurlin, and R. C. Pacanowski. Properties of long equatorial waves in models of the seasonal cycle in tropical Atlantic and Pacific Oceans. *J. Geophys. Res.*, **91**, 14207–14211, 1986.

8. J. P. McCreary and Z. Yu. Equatorial dynamics in a 2 1/2-layer model North Equatorial Countercurrent. *Prog. Oceanogr.*, **29**, 61–132, 1992.

9. S. G. H. Philander. Instability of zonal equatorial currents, 2. *J. Geophys. Res.*, **83**, 3679–3682, 1978.

10. B. G. Kelly, S. D. Meyers, and J. J. O'Brian. On the generating mechanism for yanai waves and the 25-day oscillation. *J. Geophys. Res.*, **100**, 10589–10612, 1995.

11. L. Miller, D. Randolph, and M. Wimbush. Oscillation of dynamic topography in the eastern Equatorial Pacific. *J. Phys.Oceanogr.*, **15**, 1759–1770, 1985.

12. P. J. Flament, S. C. Kennan, R. A. Knox, P. P. Niiler, and R. Bernstein. The three-dimensional structure of an upper ocean vortex in the tropical Pacific Ocean. *Nature*, **383**, 610–613, 1996.

13. J. P. Boyd. Hyperasymptotic perturbation theory and numerical studies of nonlocal solitary waves with applications to near-equatorial ocean vortices. In AMS, editor, *11th conference on Atmospheric and Oceanic Fluid Dynamics*, pages 11–12. MIT Press, 1997.

14. P. Y. Le Traon, Nadan, and Ducet. An improved mapping method of multi-satellite altimeter data. *J. Atmos. Oceanic Tech.*, in press, 1998.

15. J. P. Angell, T. R. Robinson, and S. P. Lawrence. Topex observations of Kelvin, Rossby and tropical instability waves in the Pacific Ocean. *Adv. Space Res.*, in press.

16. C. Périgaud. Sea level oscillations observed with Geosat along the shear fronts of the Pacific North Equatorial Countercurrent. *J. Geophys. Res.*, **95**, 7239–7248, 1990.

17. L. Qiao and R. H. Weisberg. Tropical instability wave kinematics: Observations from the tropical instability wave experiment. *J. Geophys. Res.*, **100**, 8677–8693, 1995.

18. M. J. McPhaden. The tropical atmosphere-ocean array is completed. *Bull. Amer. Meteor. Soc.*, **76**, 739–741, 1995.

19. R. W. Reynolds and T. M. Smith. Improved global sea surface temperature analyses using optimum interpolation. *J. Clim.*, **7**, 929–948, 1995.